Characterization of frequency effect in SuperDARN spectral width distributions

X. Vallières, J.-P. Villain, R. André

Characterization of frequency effect in SuperDARN spectral width distributions

X. Vallières, J.-P. Villain, and R. André

Laboratoire de Physique et Chimie de l'Environnement, CNRS, Université d'Orléans, Orléans, France

Received 2 November 2001; revised 29 July 2002; accepted 25 September 2002; published 7 January 2003.

[1] This study investigates the frequency dependence of spectral width distributions observed by the SuperDARN HF radars. The evolution of spectral width values with range is shown to be dependent on the operating radar frequency. First, this evolution is clearly pointed out using a multifrequency scanning mode. This study is then generalized and this effect is shown to affect the whole SuperDARN spectral width data set. Several studies are performed in order to determine the dependence of this effect upon season, beam orientation and mean radar orientation. *INDEX TERMS:* 2407 Ionosphere: Auroral ionosphere (2704); 2439 Ionosphere: Ionospheric irregularities; 2487 Ionosphere: Wave propagation (6934)

Citation: Vallières, X., J.-P. Villain, and R. André, Characterization of frequency effect in SuperDARN spectral width distributions, *Radio Sci.*, *38*(1), 1003, doi:10.1029/2001RS002550, 2003.

1. Introduction

[2] One of the main goals of SuperDARN (Super Dual Auroral Radar Network) is to obtain global convection maps of ionospheric plasma motions driven by solar-terrestrial geophysical phenomena [*Greenwald et al.*, 1995]. More and more studies are making use of spectral width values to identify auroral regions or specific magnetospheric boundaries. Indeed, these values are expected to depend on the effect of geophysical conditions determining the spectral characteristics. For example, *Baker et al.* [1990, 1995] and *Rodger et al.* [1995] have shown that spectral width exhibits particular properties within the cusp. Also, *Dudeney et al.* [1998] found a sharp latitudinal increase of the spectral width collocated with the boundary with the central plasma sheet (CPS) and the boundary plasma sheet (BPS). This increasing interest in spectral width values for identifying magnetospheric regions or boundaries by their ionospheric footprints requires that reliable data sets be provided by SuperDARN. In this study, we are specifically interested with statistical distributions of spectral width values and their dependence upon frequency and range.

[3] Previous studies [*Grésillon et al.*, 1992; *Hanuise et al.*, 1993; *Villain et al.*, 1996] have applied collective scattering theory to radar spectra in order to characterize them in terms of micro-physical processes and to relate their spectral shapes to diffusion processes. They have shown that the spectral width characteristics are related to the turbulent motions of density irregularities. *André et al.* [1998, 2000] showed a radar frequency dependence of the diffusion coefficient associated with spectral shape. However, because diffusion coefficients are expected to be constant in the 8–20 MHz SuperDARN frequency range, these authors proposed that, during propagation, a decorrelation of the wave front occurs due to interactions with larger-scale ionospheric plasma irregularities.

[4] In this paper, a more precise characterization of this effect and the generalization of its observation are conducted. Spectral width distributions are shown to reveal a radar frequency dependence. In a first part, evidence is presented of this effect using a special multifrequency sounding mode run on the Stokkseyri SuperDARN radar. Then, we show that this frequency effect is present in the whole SuperDARN data set. Particular studies show that this effect is global, does not depend on season, radar or beam orientation, and thus is independent of geophysical considerations or geometrical factors. Following *André et al.* [1998], a mechanism to understand this observation is discussed as due to decorrelation of the wave front by medium-scale ionospheric plasma irregularities.

2. SuperDARN Radars

[5] SuperDARN is an international network of coherent HF paired radars scanning the ionosphere in the northern and southern auroral zones and polar caps at frequencies ranging from 8 MHz to 20 MHz [*Greenwald et al.*, 1985, 1995]. All radars are built on the same pattern and produce similar data. Each radar field of view

0048-6604/03/2001RS002550

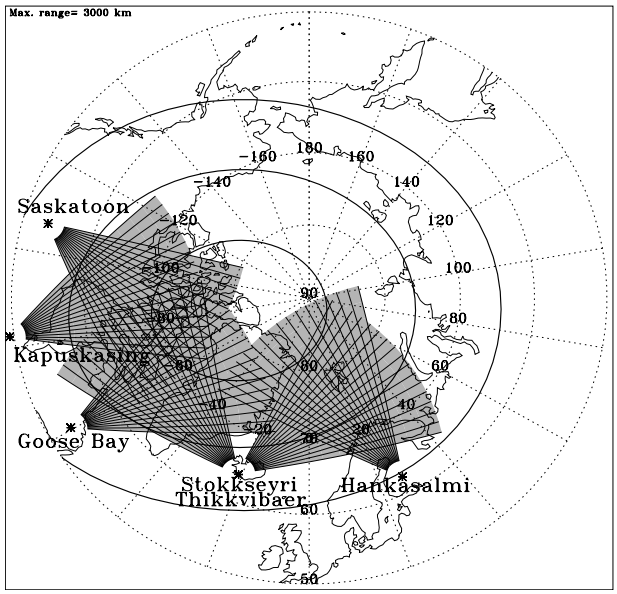

Figure 1. Location and fields of view of SuperDARN radars used in this study. The contours in thick line correspond to Invariant Latitude of 60°, 70° and 80°.

covers 70 range gates (from 180 km to 3300 km) and an azimuthal sector of 53 degrees split in 16 beams separated by 3.3 degrees. Figure 1 shows the coverage of six radars from the northern hemisphere used in this study with geomagnetic latitudes plotted as bold lines. Such radars detect the ionospheric plasma motion perpendicular to the Earth magnetic field. The transmitted radio waves are refracted in the ionosphere and can therefore reach perpendicularity with the Earth magnetic field. A small part of the energy is coherently backscattered by ionospheric structures aligned with the Earth magnetic field. The backscattered wave undergoes a Doppler frequency shift proportional to the radial component of the plasma velocity and is then received and analyzed by the radar. In order to measure both the velocity and the direction of the plasma motion in the plane perpendicular to the Earth magnetic field, the radars are paired, so that they have overlapping fields of view.

[6] Here, we only consider spectral width values as calculated by the basic algorithm. From the analysis of the complex autocorrelation function (ACF) [*Villain et al.*, 1987; *Baker et al.*, 1995], three main parameters are deduced: the power which gives the signal to noise ratio, the Doppler velocity which gives the radial component of the average velocity in the scattering volume and the spectral width which reveals the distribution of turbulent velocities present in the scattering volume in the absence of other physical constraints. These parameters are controlled both by the plasma instability mechanisms within the ionosphere, and by the large scale convective motions which are the consequence of solar wind/magnetospheric plasma coupling phenomena. A complete radar scan is performed every 2 minutes in the standard operating mode, and the three above parameters are determined for every range cell where the scattered power is above a standard threshold.

3. Case Study: Special Mode for the Stokkseyri Radar

[7] The SuperDARN HF radars operate in a continuous mode to provide measurements of ionospheric convection. Most of the operating time is devoted to common scanning modes shared by all radars. In normal scanning mode, the SuperDARN radars operate at predetermined frequencies ranging from 8 MHz to 20 MHz. Before each integration time, a receiver frequency band search is implemented to determine the quietest frequency, and the radar operates at this frequency for the integration time (usually 7 seconds). During about 20% of the operating time, the radars can run specific sounding modes called discretionary modes, designed to achieve specific scientific goals.

[8] In this study, we first use data obtained with a specific discretionary mode run on the Stokkseyri radar (see Figure 1) devoted to multifrequency ionospheric studies. This mode enables nearly simultaneous sounding at four frequencies: 9 MHz, 12 MHz, 14 MHz and 16 MHz. For each beam direction, the sounding is done for each of the four selected frequencies consecutively with a 7-second integration time. For such a frequency scan of 28-second duration, we assume that there are no spatial and temporal variations of the ionospheric variations. Data analysis is conducted using the standard method [*Villain et al.*, 1987]. Here, we consider data from January 1995 to August 2000 when this Stokkseyri specific mode was used an average of three days per month (except for 1997 for which very little time was devoted to this mode). This database contains about 4,300,000 points. The special multifrequency sounding allows to have a database in which each frequency contributes about 25% of the total data. Moreover, the data distribution for each frequency is similar with respect to range gate and beam. Figure 2 shows the frequency distribution within this database, emphasizing the very distinct and nonoverlapping frequencies used for this special mode.

[9] We come now to study the differences between the statistical distributions of Doppler spectra parameters obtained for each frequency, with a particular emphasis upon the spectral width values. Ground scatter echoes, which are characterized by low spectral width and velocity value [*Baker et al.*, 1988], have been rejected from the database. Moreover, data have been filtered out

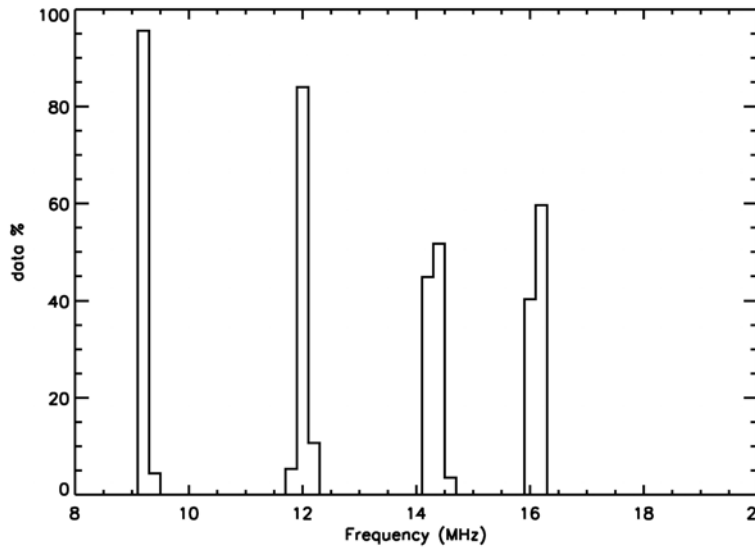

Figure 2. Frequency distribution for the database obtained with the multifrequency special mode, showing the echo occurence at the four selected frequencies, namely 9 MHz (766,739 points), 12 MHz (837,320 points), 14 MHz (784,247 points) and 16 MHz (811,287 points).

on the basis of the following criteria: echoes with power (P) lower than 7 dB and echoes with an absolute velocity (|V|) or width (W) lower than 50 m.s^{-1} are rejected. After this selection, there are about 800,000 points for each frequency range.

[10] Figure 3 presents the color-coded relative echo occurence as a function of range and power in dB for each frequency with a resolution of 45 km in range (corresponding to the radar cell length) and 1 dB in power. We note that the general shapes of each distribution are in good agreement. As can be observed on Figure 3, there are mainly two regions of echoes: the first one at near ranges (less than 1000 km, particularly dominant at 16 MHz) and the second one (with lower power values) which peaks between 1200 km and 1600 km, depending on frequency. One can also notice a shift in range of these regions between the 9 MHz and the 16 MHz distribution. Figure 4 shows the echo occurence as a function of range and spectral width (converted from the Doppler spectrum in Hz to velocities in m.s^{-1}) for each frequency, with a resolution of 45 km in range and 5 m.s^{-1} in width. Misclassification of ground scatter echoes as ionospheric echoes may lead to a mixing of both kinds of echoes and thus to specially low spectral width values in the distributions. This effect is clearly observed for the 9 MHz distribution. This low spectral width regions (less than 100 m.s^{-1}), due to noneliminated ground echoes, will be ignored from now. One can observe the two main echo regions previously discussed on Figure 3.

[11] On both Figures 3 and 4, we observe a shift towards greater ranges of the two echo regions with increasing frequency. The near-range peak is at 500 km for 9 MHz and at 650 km for 16 MHz and the far-range peak is at about 1200 km for 9 MHz while it is at 1600 km for 16 MHz. This shift is a general effect on distributions since it is also observed in the transition between the two regions. The shift in range of these regions and their transition has to be related to the refractive properties of the ionosphere and its influence on wave propagation. Lower frequency waves are more refracted and trajectories are bent more rapidly along their propagation path, so the condition of perpendicularity to the magnetic field is reached at nearer ranges. Higher frequency waves are less refracted and must propagate deeper in the ionospheric plasma before being backscattered and are associated with greater range gates.

[12] The two echo regions observed both in Figures 3 and 4 may be associated with ionospheric E and F regions as shown in numerous ray tracing studies [e.g., *André et al.*, 1997]. *Villain et al.* [1984] showed that perpendicularity to the magnetic field should be reached in the F-region for group distances between 1200 km and 2200 km. *Hanuise et al.* [1991] or *Uspensky et al.* [1994] studied data from the SHERPA radar at 6 frequencies between 9 MHz and 16 MHz and showed the influence of refraction effects. They showed that the minimum range of F-region echoes is at 700 km at 11 MHz, increasing to 1000 km at 14 MHz. On the other hand, they showed that E-region echoes are associated with nearer ranges but may be associated with ranges up to 1000 km, especially at 16 MHz. Our results are in good agreement with their findings. At intermediate ranges, the

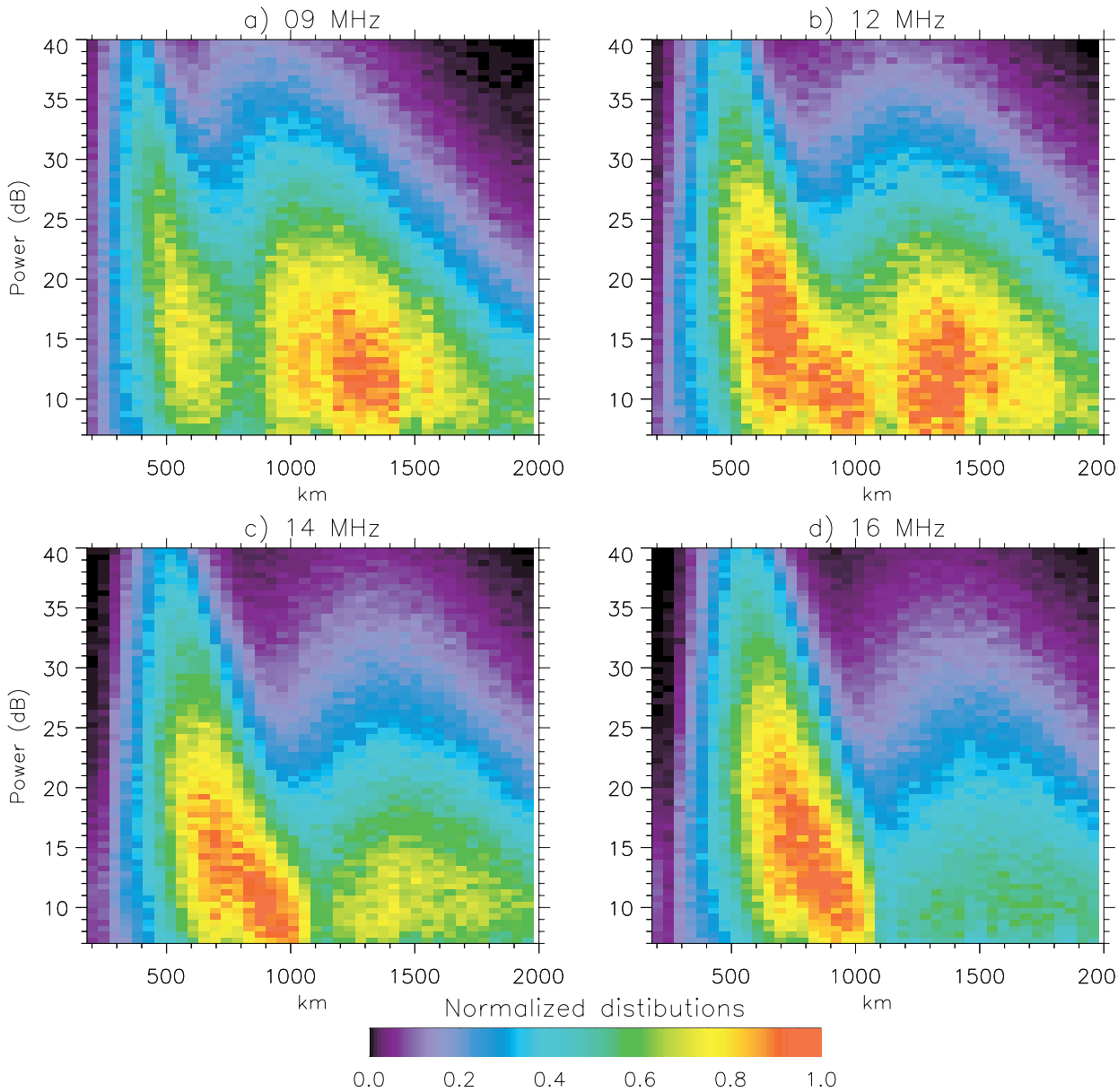

Figure 3. Data distribution as a function of power value in dB and range for the four frequencies of the multifrequency special mode: (a) 9 MHz, (b) 12 MHz (c) 14 MHz and (d) 16 MHz. Distribution for each frequency is normalized to its maximum value. The grid resolution is 45 km in range and 1 dB in power.

distinction between E-region echoes and F-region echoes may not be obvious (as shown by the overlapping of the two echo regions in Figures 3 and 4) because of the multiple modes of propagation in the ionosphere. Echoes may be coming from the ground whereas others may be originating from the E or F-regions concurrently. Composite signals of this type would have multiple spectral components and exhibit spectral broadening depending on propagation frequency. Furthermore, they likely would increase the velocity errors deduced by the basic algorithm used for SuperDARN data. Velocity errors have been analyzed for the entire database. For all frequencies, velocity errors show a slight increase of about 15 m/s with range between 300 km and 2000 km which may partially be related to the signal to noise ratio decrease with range. On the other hand, the velocity

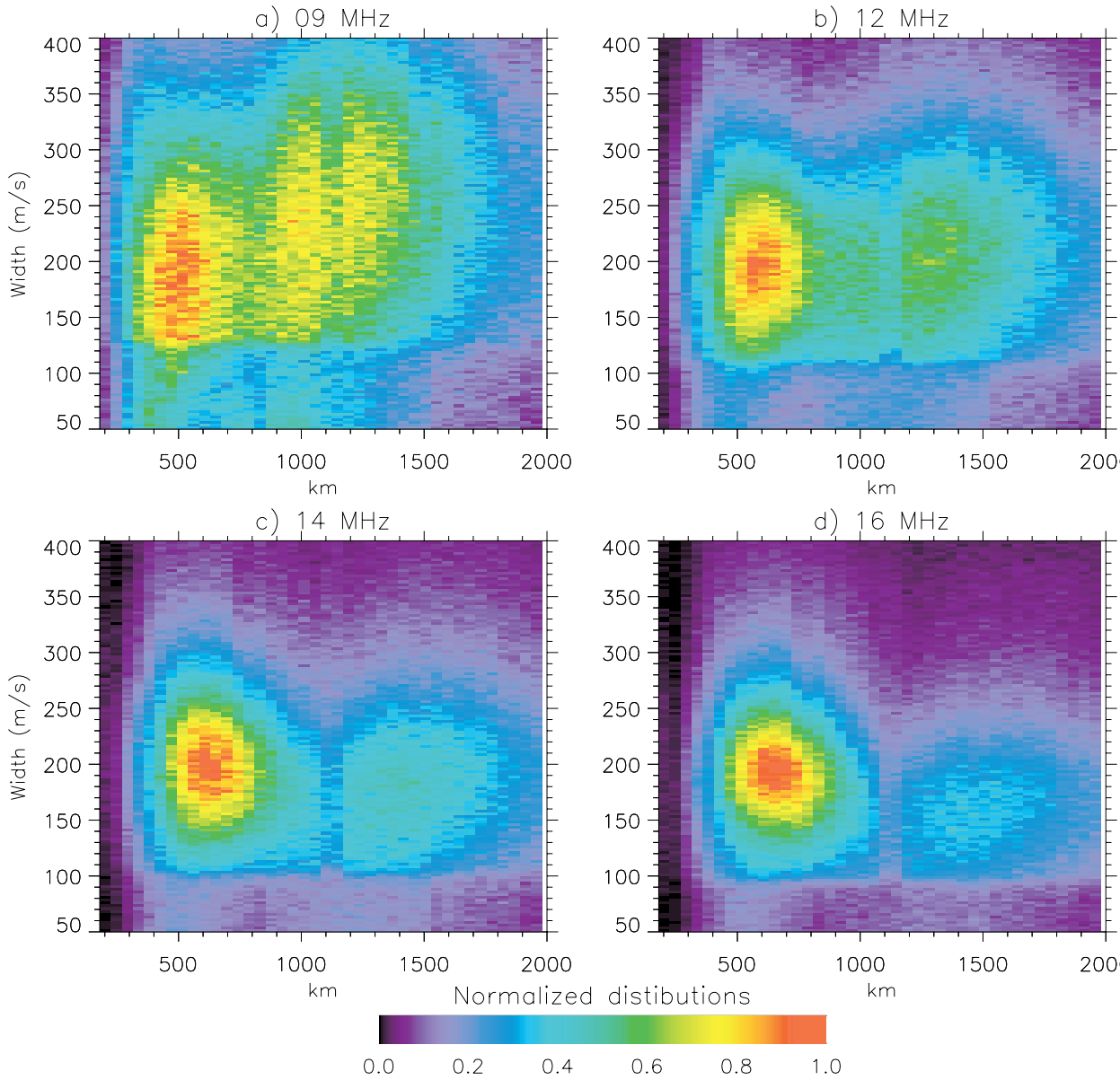

Figure 4. Data distribution as a function of spectral width value in $m.s^{-1}$ and range for the four frequencies of the special multifrequency mode: (a) 9 MHz, (b) 12 MHz (c) 14 MHz and (d) 16 MHz. Distribution for each frequency is normalized to its maximum value. The grid resolution is 45 km in range and 5 $m.s^{-1}$ in width.

errors associated with each frequency exhibit very little difference: a shift of about 10 m/s,independent of range, has been noted between velocity errors at 9 MHz and those at 16 MHz. This study demonstrates the consistency of the database and the minor influence of composite signals. The effect discussed in this paper deals with ranges lower than 2000 km for which nondirect ionospheric scatter is not the preferential propagation mode. The presence of this mode should not affect the statistical results.

[13] However, the aim of this paper is not to identify E and F-regions but to describe the evolution of data and width distributions with frequency. When looking at Figures 3 and 4, one has to notice particular ranges (around 1100 km, 1500 km) presenting discontinuities with the general shape of both power and spectral width

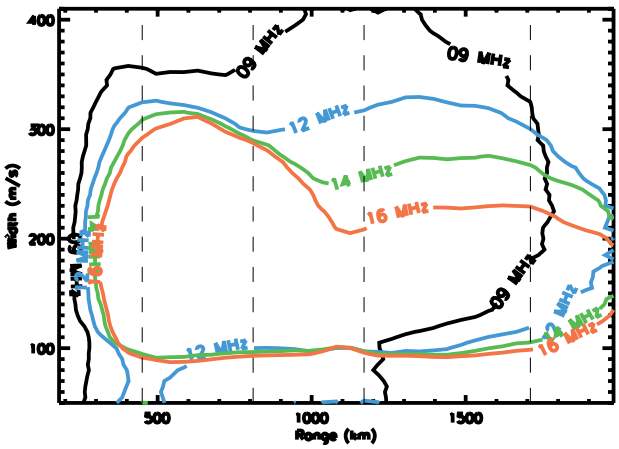

Figure 5. Contour overplot associated to distributions shown in Figure 4, for 9 MHz (black), 12 MHz (blue), 14 MHz (green) and 16 MHz (red).

distributions. These discontinuities are due to a systematic low amount of data and are associated with specific ranges independent of frequency. This low amount of data is an instrumental effect, referred as "badlags" and is due to the monostatic nature of SuperDARN radars. This effect occurs when a pulse is transmitted at the same time that the receiver should be receiving echoes from a previous pulse. Because the receiver is blanked during transmission, no signal is detected. As mentioned by *Huber* [1999], the position of badlags depends upon the transmitted pulse pattern, for the current pulse sequence used for the Stokkseyri mode and for most of the SuperDARN data used in this study, badlags occur in ranges 5 + 8n (n = 0,..,8). The range following a badlag is also affected due to the finite decay time of the pulse. For the ranges considered in Figures 3 and 4, badlags correspond to ranges: 360 km, 720 km, 1080 km, 1440 km and 1800 km. These badlags are clearly observed in Figures 3 and 4, especially for the ranges 1080 km and 1125 km. Nevertheless, this effect results in a lower data amount but does not affect the distribution shape and the different trends for each distribution, as it would be observed in the next figure.

[14] If we consider only the F-region (far-range) scatter, it is interesting to note the evolution of the four frequency distributions as a function of range. At 9 MHz, considering the general shape of the distribution, spectral width values (Figure 4) are greater than for the other frequencies and seem to increase with increasing ranges. This trend is observed but less obvious at 12 MHz. For higher frequencies, there is almost no change of the mean spectral width values with range. Figure 5 presents an overplot of contours associated with the four distributions, illustrating the frequency organization of spectral widths. Each contour is associated with a frequency and corresponds to a 35%-level of the maximum occurrence for each distribution.

[15] The width increase as a function of range is more important at 9 MHz than at 12 MHz, 14 MHz and 16 MHz. The vertical dashed lines correspond to particular ranges where cuts have been made, leading to the echo occurence as a function of spectral width for the four frequencies and for these particular ranges. In order to compare the distributions for the four frequencies, we have chosen particular values of ranges such that the first dashed line at 450 km corresponds to E-region for the four frequencies. For the second dashed line at 810 km, it can be seen from Figure 3 that it lies in the E/F overlapping region for 9 MHz, while it is most exclusively E-region for the three other frequencies. Finally, the two last dashed lines at 1170 km and 1710 km correspond to purely F-region scatter for all frequencies.

[16] These cuts are shown on Figure 6 for the four frequencies. For the first range of 450 km, the distributions exhibit the same characteristics, peaking at spectral width values of about 150 m.s^{-1}. The 9 MHz distribution is somewhat broader due to normalization but does not exhibit a shift in average width. With increasing values of range, the four distributions split, giving rise to a frequency separation of the distributions. For the second selection of range of 810 km, the 12 MHz, 14 MHz and 16 MHz distributions are identical and similar to the distribution at 450 km while the distribution for 9 MHz starts already to split due to the presence of F-region scatter. At a range of 1710 km, the 9 MHz distribution peaks at about 230 m.s^{-1} whereas the 16 MHz distribution peaks at only 150 m.s^{-1} then producing a shift as important as 80 m.s^{-1} in average. One can also notice that between 1170 km and 1710 km, the 9 MHz distribution shows little variation while the 12 MHz, 14 MHz and 16 MHz distributions increase in mean. This evolution confirms the frequency separation with range, except for the 9 MHz distribution, for which the frequency effect seems to saturate. For each frequency, the width distribution is processed in order to deduce the mean value and standard deviation for each range. Figure 7 shows the evolution of the width mean value (solid line) associated with each frequency distribution as a function of range. Dashed lines correspond to the evolution of the standard deviation added to the width mean value, and to the evolution of the standard deviation subtracted to the width mean value. This figure again illustrates the difference observed between the near-range and far-range region. For ranges lower than 1000 km, the four frequency distributions exhibit very similar characteristics, with a spectral width value of about 200 m.s^{-1}. For greater ranges, one can notice an increase of the width mean value with increasing range. The evolution of standard deviation does not seem to play a significant role with regards to frequency, as shown by the evolution

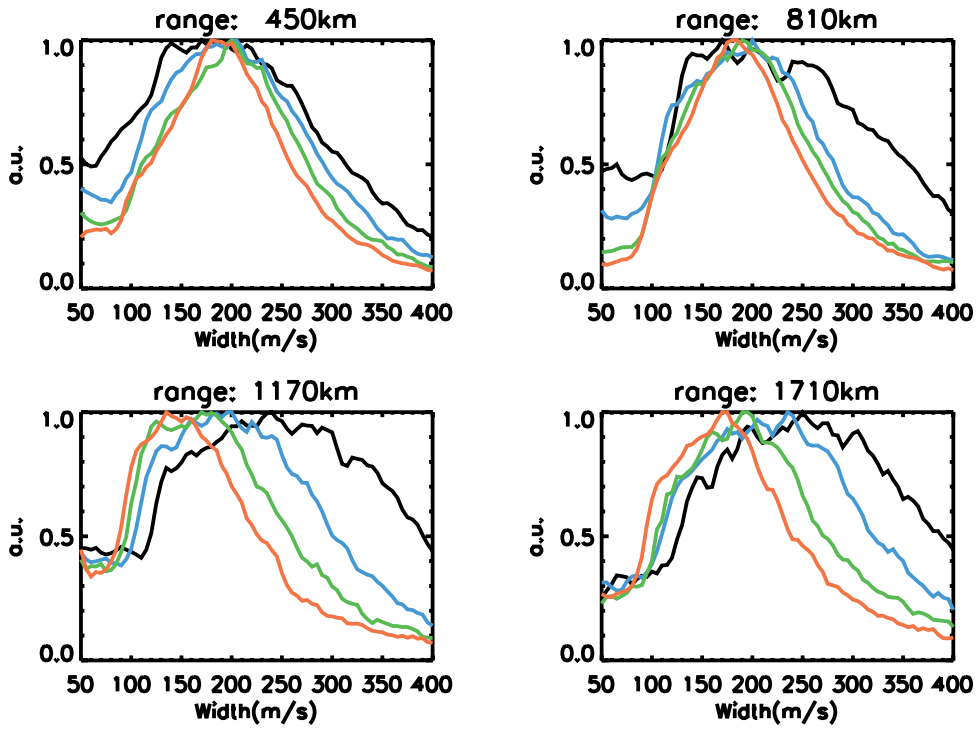

Figure 6. Cuts of distribution for 9 MHz (black), 12 MHz (blue), 14 MHz (green) and 16 MHz (red), given for ranges of 450 km (a), 810 km (b), 1170 km (c) and 1710 km (d).

of dashed lines. More precisely, width distributions do not broaden with range, so that the frequency effect discussed here is not due to any distribution broadening with range or frequency. For the 9 MHz distribution, spectral width reaches a plateau around 1500 km. For 12 MHz, a plateau is reached as well but for greater ranges, around 1700 km, while no such plateau is observed for higher frequencies up to 2000 km. This feature may be associated with a saturation process with range which occurs at near ranges at 9 MHz than for higher frequencies. At very far ranges, it also reduces somewhat the difference between the spectral width at 9 MHz and those obtained at higher frequencies. We note that at these ranges, the difference between the 9 MHz distribution and the 16 MHz distribution is reduced to approximately 50 $m.s^{-1}$ for spectral width mean values.

[17] Several studies have been performed to show the generality of this effect. In order to consider the role of particular events, distributions have been studied for reduced databases obtained by considering half of the total data amount. The previously described frequency effect was observed for these databases, then leading to an interpretation in terms of a general effect and not of particular propagation or ionospheric conditions. This effect has also been tested with data from different seasons (winter, summer and equinox) and has been shown to be independent of seasonal effects.

[18] Another kind of study has been performed, regarding the influence of beam orientation. Indeed, the Stokkseyri radar is magnetically oriented in such a way that its first beams are zonal beams, i.e. oriented along the east-west direction whereas the last beams are more meri-

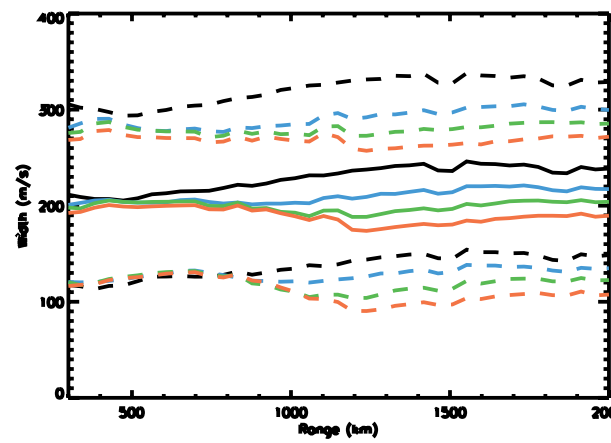

Figure 7. Spectral width mean value (solid line) and standard deviation (dashed line) added to and subtracted from the width mean value as a function of range for 9 MHz (black), 12 MHz (blue), 14 MHz (green) and 16 MHz (red).

dional i.e. more nearly aligned with the magnetic meridian (see Figure 1), so that physical parameters extracted from echoes from the first or last beams are greatly influenced by the global ionospheric convection pattern and propagation condition effects. However, echoes from the first and the last beams have been shown to have very similar distributions with range and spectral width for each frequency respectively. Therefore, we can interpret the frequency dependence of these distributions as independent of large-scale global convection pattern or propagation conditions.

[19] Highlighting the frequency effect for different seasons also show that the spectral width-frequency effect is independent of the season and therefore of the changing seasonal factors affecting the ionospheric turbulence. This effect should be present in even more global databases.

4. Global Study

[20] This section is dedicated to a study, for the whole SuperDARN database, of the previously described frequency effect on spectral width evidenced with the multi-frequency specific program run on the Stokkseyri radar.

4.1. Whole SuperDARN Database Overview

[21] We have considered data from 6 radars of the northern hemisphere operating in a common normal scanning mode, for which operating frequencies are independent for each radar (theoretically between 8 MHz and 20 MHz). In contrast to the previous analysis, based upon the special discretionary mode used on the Stokkseyri radar, echoes at different frequencies are not obtained sequentially, but our purpose here is to give evidence that the spectral width distributions are statistically influenced by the operating radar frequency and not to show quantitative results as in the previous section. Theoretically, sounding frequencies range from 8 MHz to 20 MHz; however, radars usually operate with frequencies near 10 MHz or higher. Identified ground scatter echoes were systematically eliminated and only echoes associated with ranges greater than 900 km i.e. associated to the F-region were considered. Echoes were obtained from normal scanning mode periods between November 1995 and August 1998, representing a total of about 60,000,000 points. Echoes have been filtered out following the same criterion as in the previous study ($|V| > 50$ m.s^{-1}, $W > 50$ m.s^{-1}, $P > 7$ dB). Parameter distributions are given as a function of magnetic local time (MLT) and magnetic latitude (MLAT). The grid resolution is arbitrarily chosen of 30 minutes in MLT and 1 degree in MLAT. For each cell (corresponding to a particular MLT and MLAT), distributions of echo parameters have been computed. We present here the mean value of spectral width distribution for each cell, thus giving a representation of its global distribution as a function of magnetic latitude and magnetic local time.

4.2. Spectral Width Distributions

[22] Using the normal scanning mode as compared to the Stokkseyri specific mode described in the previous section is much more stringent due to the fact that the frequency is more restricted and does not vary as much as for the specific mode run on Stokkseyri radar (9 MHz-16 MHz). We split the echoes into two ranges of frequency: frequencies greater than 10 MHz and frequencies lower than 10 MHz.

[23] Figure 8 shows color-coded data distributions in a MLT-MLAT frame for frequencies greater than 10 MHz (a) and for frequencies lower than 10 MHz (b), considering the whole data set. In this figure, the purpose is not to discuss specific features appearing in the spectral width distribution. Such MLT-MLAT distribution of spectral width has been related to the footprint of magnetospheric regions either through case studies [e.g., *Baker et al.*, 1986] or statistical analysis [e.g., *Villain et al.*, 2002; *André et al.*, 2002]. But we wish to point out the systematically greater spectral widths observed on the distribution corresponding to frequencies lower than 10 MHz. Local maxima are located approximately in a 09–12 MLT and 75°–80° MLAT sector on both plots. One noticeable point is the good general agreement of both distributions exhibiting the same global shape with respect to magnetic local time and magnetic latitude, but with a systematic enhancement of the spectral width for frequencies lower than 10 MHz. This inverse relationship between spectral width and frequency is thought to be related to the previous frequency effect: for F-region echoes, spectral width values are expected to be more important for lower frequencies. This 6-radar study shows that this effect depends neither on radar location nor on field of view orientation. In order to confirm this trend, similar studies were made based upon the mean orientation of the radars. Indeed, two of the radars considered are rather zonal radar (Iceland radars: Stokkseyri and Thikkvibaer, see Figure 1) whereas the other radars are more meridional radars. Figure 9 illustrates this study, showing that the increase in spectral width values with decreasing frequency is also present for meridional radars. The same kind of study for meridional radars shows that whichever orientation is considered, spectral width values for lower frequencies are again greater.

[24] As for the Stokkseyri specific mode study, we investigated the seasonal dependence. Obviously, the global spectral width distribution is expected to depend on geophysical effects and energy source localization due in particular to solar activity and also to seasonal effects leading to differences of the global distribution between different seasons. What is investigated here are differ-

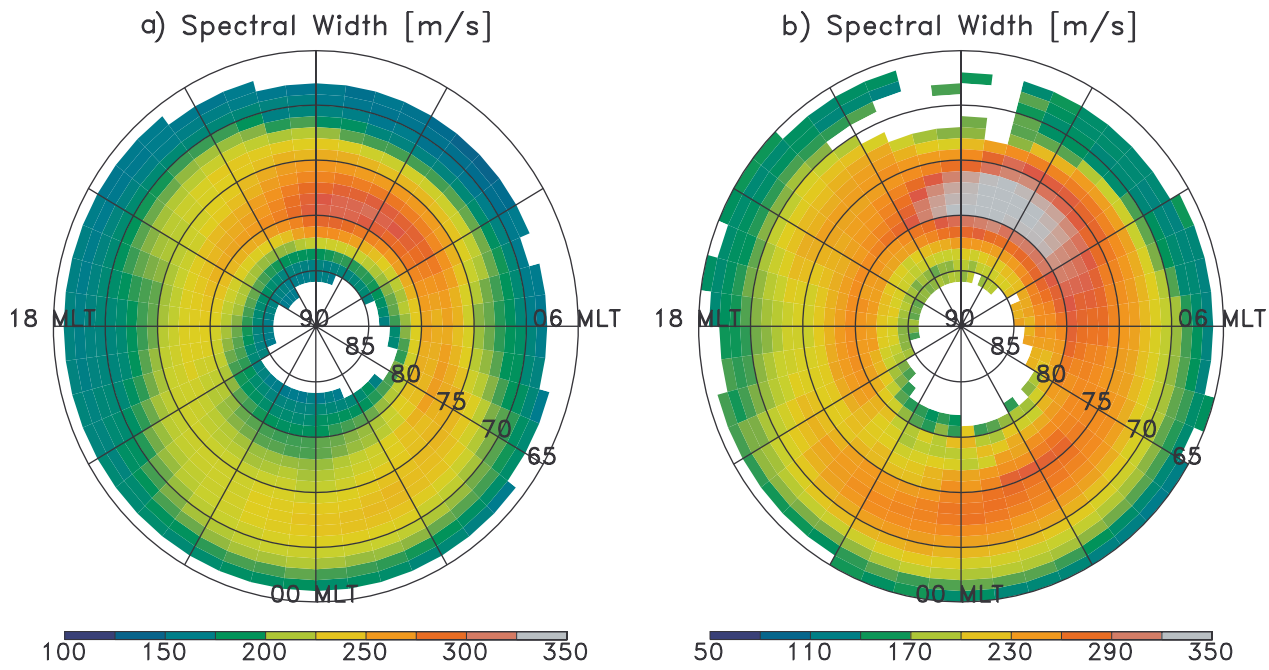

Figure 8. Statistical distribution of spectral width values for frequencies greater (a) and lower (b) than 10 MHz in a MLT-MLAT reference frame, with a grid resolution of 30 minutes (MLT) and 1° (MLAT).

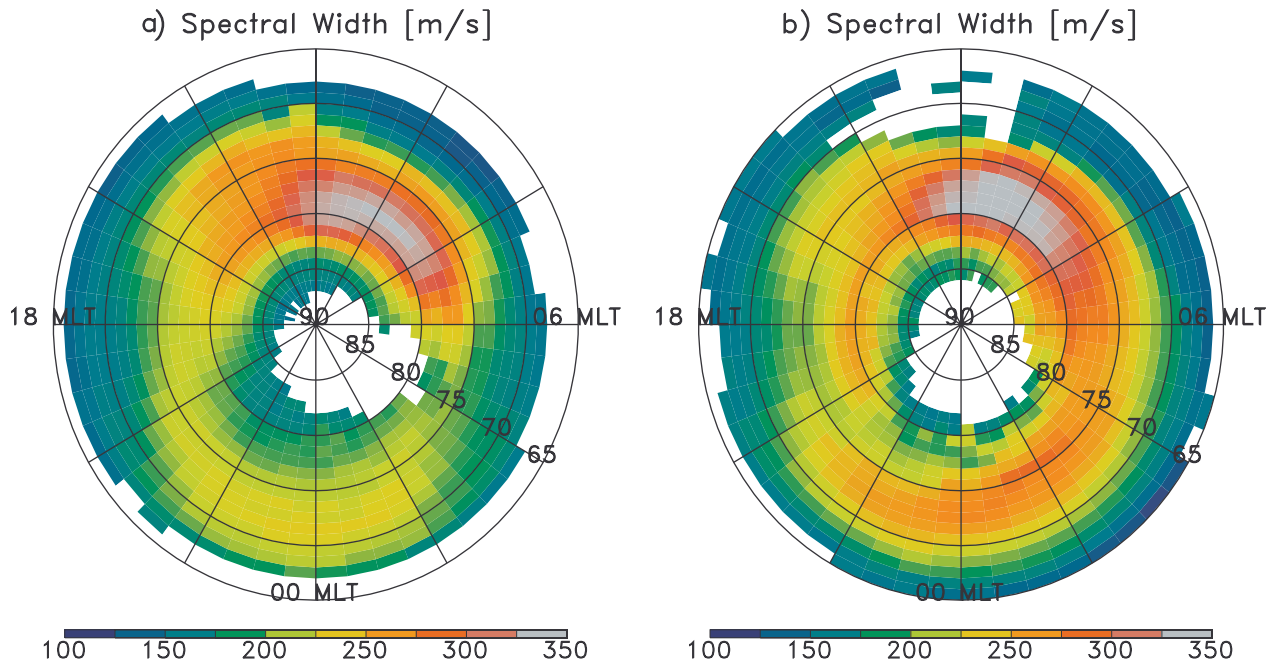

Figure 9. Statistical distribution of spectral width values for frequencies greater (a) and lower (b) than 10 MHz for meridional radars in a MLT-MLAT reference frame, with a grid resolution of 30 minutes (MLT) and 1° (MLAT).

ences between frequencies for each season considered. Three seasons were examined: summer (May - June - July - August), winter (November - December - January - February) and equinox (March - April - September - October); in each case, it was found that spectral width values for lower frequencies are greater than those for higher frequencies whereas the global shape of distributions for both frequencies shows good agreement.

[25] More specific studies were driven mixing the two former considerations: seasonal effects and radar orientation. The study of spectral width distributions for each season and each orientation does not show any evidence of disagreements with the previously observed effect.

[26] The 6-radar database analysis shows that the influence of radar frequency on spectral width distributions is spatially extensive, season independent and beam orientation independent. This conclusion shows that global geophysical effects cannot be given for responsible for the frequency dependence effect observed.

5. Discussion and Conclusions

[27] Using a ground-based HF multifrequency sounding of the auroral ionosphere, it has been shown that the evolution of the spectral width values from the Doppler spectrum (associated with the distribution of turbulent velocities within the sounded cell) with range depends on the operating radar frequency. The ionospheric near-range region echoes seem not to be affected by such an effect. Considering the middle-range region, from about 900 km to 1400 km, the spectral width values increase quasi linearly with range for the two lowest frequencies while the effect is not obvious for higher frequencies. At far ranges, this effect saturates at low frequencies while the spectral width values start to increase with range for higher frequencies.

[28] Such an effect may lead to differences between mean spectral width values at 9 MHz and 16 MHz of up to 80 $m.s^{-1}$ at middle ranges, reduced to about 50 $m.s^{-1}$ at far ranges, due to the saturation process.

[29] This effect has been shown with a special multi-frequency mode run on the Stokkseyri radar. It has been observed to be a general effect and shown to affect all six of the northern hemisphere radars used in this study, based upon data from nearly three years. This effect has been identified as spatially extensive, independent of radar or beam orientation and affecting spectral width distributions for every season.

5.1. Geometrical Effect

[30] The evolution of spectral width values with range leads us to propose an interpretation in terms of a propagation effect. One has to take care of other effects able to affect spectral width values when changing the radar frequency. For example, the beam width of the radar wave is known to be affected by radar frequency. Indeed, increasing the radar frequency results in reducing the beam width then leading to smaller cell typical size at higher frequencies. Nevertheless, this effect should influence all ranges whereas the frequency effect discussed in this paper is not seen at near ranges, in the E-region. This can be explained if the E-region is characterized by a distribution of turbulent velocities whose scale sizes are considerably less than the size of the range cell. In that case, the size of the cell should not affect the measurement of spectral width. More quantitatively, for example if one considers this combined frequency-range effect, one comes to approximately a factor 5 in cell size between 16 MHz at 300 km and 12 MHz at 1000 km. For these two cells, the spectral width is rigourously identical while for a given frequency, the cell size increases only by a factor 2 between 1000 km and 2000 km. However, the global convection pattern will create inhomogeneous turbulent regions where the measured spectral width may depend on the radar cell size. The induced effect on spectral width values thus depends on the convection pattern whereas the frequency effect described in this study is shown to be independent of this pattern.

5.2. Irregularities Scale Length Effect

[31] Changing the radar frequency also affects the characteristic scale length of the irregularities which backscatter the wave. Indeed, coherent or Bragg scattering occurs when the irregularity scale length is equal to half the radar wavelength, in the backscatter mode. Therefore, shifting the radar frequency from 9 MHz to 16 MHz will result in a shift of turbulence scales from about 17 m to about 9 m. This shift in turbulence scale is not expected to have a major influence on spectral width values observed at both frequencies. In the cascading turbulent process which is supposed to govern the scanned turbulent medium, increasing the frequency will result in scatter from shorter spatial scales of turbulence. For a power law type spectrum of density fluctuations, this may induce a lower echo amplitude but the turbulent velocity distribution should not change substantially in the considered frequency regime.

5.3. Wave Front Decorrelation

[32] One way of interpretation is to consider propagation effects within the turbulent ionosphere up to the point where the scattering occurs. These propagation effects can be expressed in terms of interactions between the radar wave front and the turbulent ionosphere.

[33] In such problems, several scale lengths of variation for the refractive index are present and lead to different effects.

1. Large spatial scales of refractive index fluctuations are associated with refraction and will deviate the wave. This phenomenon enables waves to achieve perpendicularity in the ionosphere, as shown by ray tracing calculations [*Jones and Stephenson*, 1975], and has been applied to SuperDARN radar conditions [*Villain et al.*, 1984].

2. On the other hand, small spatial scales (of the order of the wavelength or smaller) result in a more isotropic angular distribution of scatter, and are at the source of the signal detected by the radar.

3. Intermediate spatial scales (of the order of few hundred meters up to the radar cell size) will deviate the wave mainly in the forward direction and will lead to amplitude and phase fluctuations of the incident wave which can be thought of as a wave front decorrelation. The effect of such ionospheric turbulent scales on wave characteristics as been studied in scintillation studies [e.g., *Crane*, 1977] as well as in radar applications [*Uspensky et al.*, 1993]. But to our knowledge, the effect of such scales on Doppler spectral width has never been reported.

[34] The interaction of the radar signal with the ionosphere depends on the propagation length of the incident wave within the turbulent medium. Moreover, it depends upon the radar frequency and plasma frequency of the medium. Indeed, as is well known from the magneto-ionic theory, for a given electron density, the refractive index is proportional to the square of the ratio of the plasma frequency to signal frequency. Hence, this interpretation shows that a decorrelation of the wave front, which increases with the propagation length, is most effective for a radar frequency close to the plasma frequency. Considering that the mean ionospheric plasma frequency is of the order of 5–7 MHz, this effect will be at least three times greater for 9 MHz than for 16 MHz. Furthermore, considering that echoes from the E-region are produced at low altitudes where the propagation distance within the ionosphere is small, the wave front will not be largely distorted by the decorrelation effect, so the spectral width of E-region echoes will suffer little variation in the considered frequency band, as observed. A quantitative description of this interpretation, using wave propagation theories through turbulent medium, is in progress and will be the subject of a forthcoming paper.

[35] **Acknowledgments.** The operation of the SuperDARN radars in the northern hemisphere used in this study is supported by the national funding agencies of the United States, Canada, the United Kingdom, and France.

References

André, R., C. Hanuise, J.-P. Villain, and J.-C. Cerisier, HF radars: multi-frequency study of refraction effects and localization of scattering, *Radio Sci.*, *32*, 153–168, 1997.

André, R., D. Grésillon, C. Hanuise, and J.-P. Villain, Auroral ionosphere plasma turbulence transport coefficient: Direct observations from radar coherent backscattering, in *1998 International Congress on Plasma Physics*, vol. 22, edited by P. Pavlo, pp. 1126–1129, Eur. Phys. Soc., Prague, 1998.

André, R., M. Pinnock, J.-P. Villain, and C. Hanuise, On the factor conditioning the Doppler spectral width determined from SuperDARN HF radars, *Int. J. Geomagn. Aeron.*, *2*(1), 77–86, 2000.

André, R., M. Pinnock, J.-P. Villain, and C. Hanuise, Influence of magnetospheric processes on winter HF radar spectra characteristics, *Ann. Geophys.*, in press, 2002.

Baker, K. B., R. A. Greenwald, A. D. M. Walker, P. F. Bythrow, L. J. Zanetti, T. A. Potemra, D. A. Hardy, F. J. Rich, and C. L. Rino, A case study of plasma processes in the dayside cleft, *J. Geophys. Res.*, *91*, 3130–3144, 1986.

Baker, K. B., R. A. Greenwald, J.-P. Villain, and S. Wing, Spectral characteristics of high frequency (HF) backscater for high latitude ionospheric irregularities: Preliminary analysis of statistical properties, *Tech. Rep. RADC-TR-87-204*, Rome Air Dev. Cent., Griffis Air Force Base, N.Y., 1988.

Baker, K. B., R. A. Greenwald, J. M. Ruohoniemi, J. R. Dudeney, and M. Pinnock, Simultaneous HF-radar and DMSP observations of the cusp, *Geophys. Res. Lett.*, *17*, 1869–1872, 1990.

Baker, K. B., J. R. Dundeney, R. A. Greenwald, M. Pinnock, P. T. Newell, A. S. Rodger, N. Mattin, and C.-I. Meng, HF radar signatures of the cusp and low-latitude boundary layer, *J. Geophys. Res.*, *100*, 7671–7695, 1995.

Crane, R. K., Ionospheric scintillation, *Proc. IEEE*, *65*, 180–199, 1977.

Dudeney, J. R., A. S. Rodger, M. P. Freeman, J. Pickett, J. Scuder, G. Sofko, and M. Lester, The nightside ionospheric response to IMF B_y changes, *Geophys. Res. Lett.*, *25*, 2601–2604, 1998.

Greenwald, R. A., K. B. Baker, R. A. Hutchins, and C. Hanuise, An HF phased-array radar for studying small-scale structure in the high-latitude ionosphere, *Radio Sci.*, *20*, 63–79, 1985.

Greenwald, R. A., et al., DARN/SuperDARN: A global view of the dynamics of high-latitude convection, *Space Sci. Rev.*, *71*, 761–796, 1995.

Grésillon, D., et al., Collective scattering of electromagnetic waves and cross-B plasma diffusion, *Plasma Phys. Controlled Fusion*, *34*, 1985–1991, 1992.

Hanuise, C., J. P. Villain, J. C. Cerisier, C. Senior, J. M. Ruohoniemi, R. A. Greenwald, and K. B. Baker, Statistical sutdy of high-latitude E-region doppler spectra obtained with the SHERPA HF radar, *Ann. Geophys.*, *9*, 273–285, 1991.

Hanuise, C., J.-P. Villain, D. Grésillon, B. Cabrit, R. A. Greenwald, and K. B. Baker, Interpretation of HF radar ionospheric Doppler spectra by collective wave scattering theory, *Ann. Geophys.*, *11*, 29–39, 1993.

Huber, M., HF radar echo statistics and spectral studies using SuperDARN, M.A. thesis, Univ. of Saskatchewan, Saskatoon, Sask., Canada, 1999.

Jones, R. M., and J. J. Stephenson, A versatile three dimensional ray tracing program for radio waves in the ionosphere, *Tech. Rep. OT 75-76*, Off. of Telecommun., U.S. Dep. of Commer., Boulder, Colo., 1975.

Rodger, A. S., S. B. Mende, T. J. Rosenberg, and K. B. Baker, Simultaneous optical and HF radar observations of the ionospheric cusp, *Geophys. Res. Lett.*, *22*, 2045–2048, 1995.

Uspensky, M. V., A. V. Kustov, G. J. Sofko, J. A. Koehler, and J. C. Foster, An alternative look at the aspect sensitivity of auroral radar backscatter: A forward scatter effect, *J. Geophys. Res.*, *98*, 7721–7728, 1993.

Uspensky, M. V., A. V. Kustov, G. J. Sofko, A. Koehler, J. P. Villain, C. Hanuise, J. M. Ruohoniemi, and P. J. S. Williams, Ionospheric refraction effects in slant range profiles of auroral HF coherent echoes, *Radio Sci.*, *29*, 503–517, 1994.

Villain, J.-P., R. Greenwald, and J. Vickrey, HF ray-tracing at high-latitude using measured meridional electron density distributions, *Radio Sci.*, *19*, 359–374, 1984.

Villain, J.-P., R. A. Greenwald, K. B. Baker, and J. M. Ruohoniemi, HF radar observations of E region plasma irregularities produced by oblique electrom streaming, *J. Geophys. Res.*, *92*, 327–342, 1987.

Villain, J.-P., R. André, C. Hanuise, and D. Grésillon, Observation of the high latitude ionosphere by HF radars: Interpretation in terms of collective wave scattering and charac-terization of turbulence, *J. Atmos. Terr. Phys.*, *58*, 943–958, 1996.

Villain, J.-P., R. André, M. Pinnock, R. A. Greenwald, and C. Hanuise, Statistical study on spectral width from SuperDARN coherent radars, *Ann. Geophys.*, in press, 2002.

R. André, X. Vallières, and J.-P. Villain, Laboratoire de Physique et Chimie de l'Environnement, Centre National de la Recherche Scientifique, Université d'Orléans, 3A, Av. de la Recherche Scientifique, 45071 Orléans cedex, France. (valliere@cnrs-orleans.fr)